JOURNAL OF QUATERNARY SCIENCE (1996) 11 (6) 495–510

CCC 0267-8179/96/060495–16

A Late Quaternary catastrophic flood in the Lahul Himalayas

PETER COXON Department of Geography, Trinity College, Dublin, Ireland
LEWIS A. OWEN Department of Geography, Royal Holloway, University of London, Egham TW20 0EX, England
WISHART A. MITCHELL School of Geological and Environmental Sciences, University of Luton, Luton LU1 3JU, England

Coxon, P., Owen, L.A. and Mitchell, W.A. 1996. A Late Quaternary catastrophic flood in the Lahul Himalayas. *Journal of Quaternary Science*, **Vol. 11**, pp. 495–510. ISSN 0267-8179

Received 6 March 1996 Accepted 8 May 1996

ABSTRACT: Impressive flood deposits are described resulting from a catastrophic lake outburst in the Upper Chandra valley in the Lahul Himalaya, northern India. Reconstructions of the former glacial lake, Glacial Lake Batal, and the discharges were undertaken using landforms and sediment data. The glacial dam burst released 1.496 km^3 of water in 0.72 days, with peak discharges of between 21 000 and 27 000 m^3 s^{-1} at Batal. Dating by OSL suggests the flood occurred ca. 36.9 ± 8.4 to 43.4 ± 10.3 ka ago. This cataclysmic flood was responsible for major resedimentation and landscape modification within the Chandra valley.

KEYWORDS: Himalayas; high-magnitude flood event; northern India; glacial lake outburst; glacial geomorphology.

Introduction

Catastrophic outbursts of glacial lakes in the Himalayas have been described by several authors (Mason 1929, 1930; Hagen *et al.*, 1963, Hewitt, 1964, 1982; Gansser, 1966; Batura Investigation Group, 1976; Fort and Freytet, 1982; Xu, 1985; Galay, 1986; Ives, 1986; Vuichard and Zimmermann, 1986, 1987). The threat of such events has been highlighted in recent years as the progressive retreat and thinning of Himalayan glaciers during the past century (Mayewski and Jeschke, 1979; Mayewski, *et al.* 1980) has resulted in the formation of new moraine-dammed lakes, and/or the enlargement of pre-existing ones between the retreating glacier front and the most recent moraines (Ives and Messerli, 1989). Small ponds on the surface of lower glacier tongues have also been noted to be enlarging and coalescing. It is, therefore, important to consider the potential effects of such catastrophic events in terms of hazard assessment, their role in the formation and destruction of landforms and their role in resedimenting valley deposits, both within the mountains and on the Indo-Gangetic Plain (cf. Burbank, 1983; Desio and Orombelli, 1983). Despite this, little research has been undertaken on the sediments and landforms that have been produced during extreme flood events. This paper will, therefore, describe the deposits and landforms that were produced during a catastrophic glacial lake outburst which occurred during Late Quaternary times in the Upper Chandra valley, Lahul Himalaya, northern India (Fig. 1). The effects of this flood can be used as an analogue to compare the likely consequences of a future dam burst in other areas of the Himalayas.

The study area

The flood deposits occur as extensive but discontinuous sheets of bouldery diamicton between Batal and Chhatiru in the upper Chandra valley (Fig. 1). The deposit is absent in some areas where glaciers have advanced into the main valley during Holocene times and removed sediments. For example, there are no flood deposits where the Bara Shigri Glacier advanced across the Chandra valley during the late nineteenth century (Fig. 1) (Mayewski and Jeschke, 1979; Mayewski *et al.*, 1980).

Figure 2 shows a geomorphological map of the flood deposits for the area around Batal. During the Last Glacial the Batal Glacier blocked the valley to form an extensive lake, Glacial Lake Batal, which backed up the Chandra valley for about 14 km (Owen *et al.*, 1996). Shorelines and deltas associated with this lake are shown in Figs 3 and 4. Dates obtained by OSL using delta sediments from the valley give an age of 43.4 ± 10.3 ka and 36.9 ± 8.4 ka (Owen *et al.*, in preparation), suggesting that the lake formed in the last cold stage, possibly during Oxygen Isotope Stage 3. A reconstruction of Glacial Lake Batal is shown in Fig. 5. Four study areas were mapped at a scale of 1 : 10 000 to show the characteristics of the flood deposits and the positions of selected transects and sampling points (Figs 5, 6, 7 and 8). In each of the study areas, the sedimentology was recorded and the a-, b- and c-axes of the five largest boulders were measured (mean diameter $(LIS)^{0.3}$) at intervals of appropriately 25–30 m along selected cross-valley transects (Figs 6 and 7; Table 1).

Figure 9 shows the characteristics of the flood deposits at selected locations. The boulders are generally imbricated

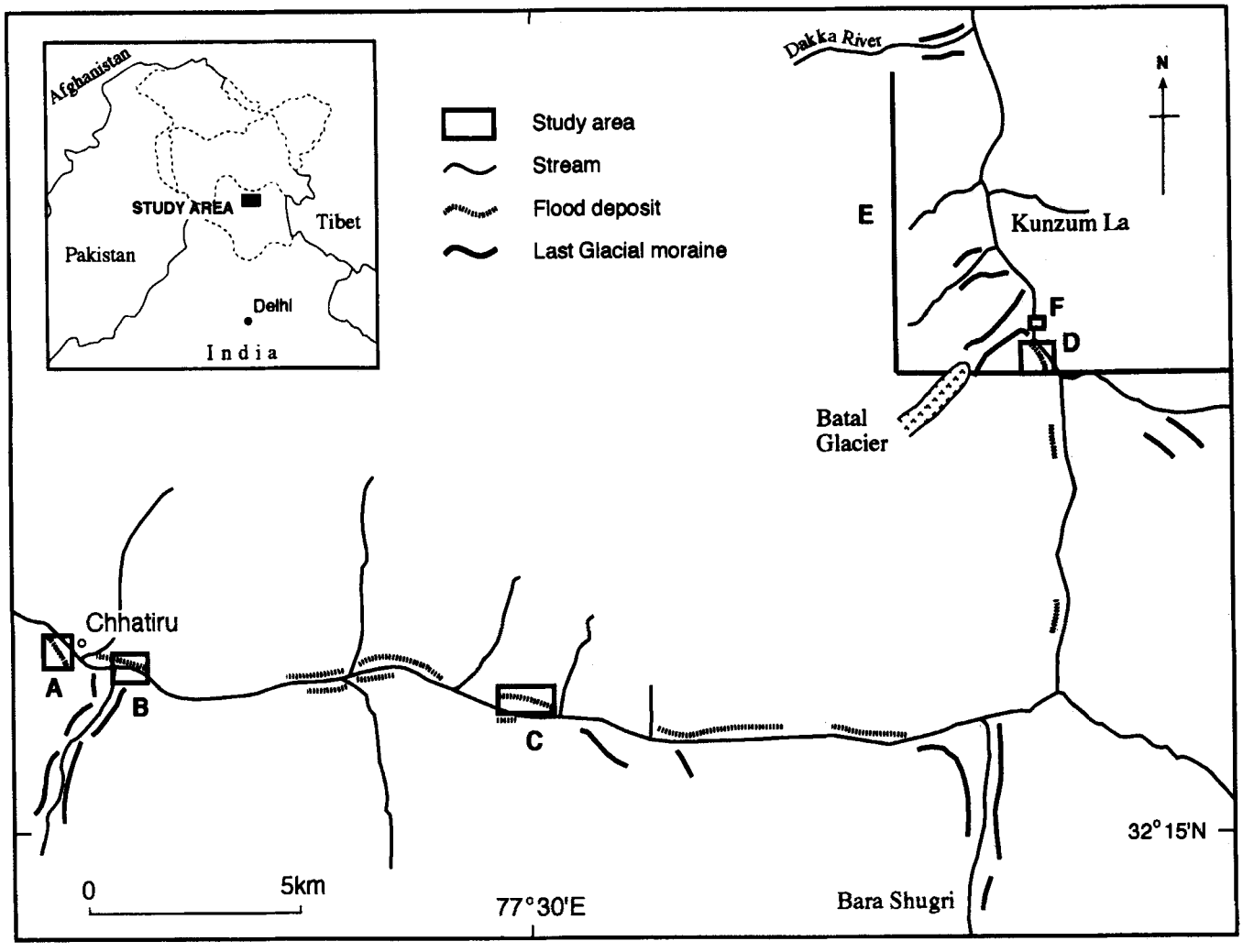

Figure 1 Map of the study area and the extent of the flood deposits. Study areas A, B and C are shown in Fig. 7, study area D is shown in Figs 2 and 6, study area E is shown on Fig. 3 and study area F is shown on Fig. 8.

and at some locations the boulders exceed 10 m in diameter. The boulders commonly form large longitudinal boulder clusters, whereas the intervening areas comprise small boulders and cobbles associated with sand lags and channels. Each area of the discontinuous flood deposit generally coarsens down-valley, suggesting that the flood comprised a series of pulses of sedimentation induced by constrictions produced by the large end moraine complexes.

The most detailed work was undertaken at Batal (Figs 2, 6 and 8). Here a series of terraces are present at heights of between 4 and 6 m above the floodplain and can be divided into two identifiable components: the floodplain terraces (which have two components); and the Batal Flood terrace upstream of the road bridge at Batal, is a small, flat, steeply dipping terrace fragment which is immediately downstream from the small moraine ridge formed by the Batal Glacier (Fig. 8). This ridge and a similar one up-valley marks the location of the former ice-dam and the limit of Glacial Lake Batal (Figs 5, 6 and 8).

The main terrace fragment (Batal Flood terrace) at Batal is 1.5 km long and up to 600 m wide (Fig. 2). To the southwest it has a broad flat area dominated by silt, which probably represents a backwater area during the flood. The terrace surface gradient steepens downstream from 1 to 3°. The sediment is, in part, a normally graded boulder and cobble gravel, but the overall clast size increases downstream.

The Batal flood terrace can be divided broadly into three zones (Fig. 6). From furthest upstream these include:

1. (0–300 m downstream from the Batal Bridge). A planar surface that is covered with occasional boulders >2–3 m in diameter, some of which have shallow scours (4–10 m long, 2–3 m wide and 0.5–1 m deep) behind them and some small ripples with decimetre-size wavelengths and centimetre-size amplitudes (area A, Fig. 6). The largest clast sizes (mean diameter $(LIS)^{0.3}$) is approximately 1.8 m.
2. (300–700 m from the Batal Bridge). The terrace is composed of cobbles and gravel which have undergone periglacial modification (clast sorting). Large wavelength ripples (17 m) with low amplitude (1 m) are present in this zone (Fig. 9C). Larger scours are present at the upstream end of this section, some are 8 m wide and more than 2 m deep (Fig. 9B). These have asymmetric tails, with a longer western side (valley side), indicating a flow direction to the southwest. Large imbricate boulders become common, with the largest clast sizes (mean diameter $(LIS)^{0.3}$) being approximately 1.92 m (Fig. 9E; area 4, Fig. 6).
3. (700–1500 m from the Batal Bridge). This part of the terrace is variable across its width and can be divided into three zones.

(i) This represents a wide backwater area of finer sediment to the west (area 5, Fig. 6).

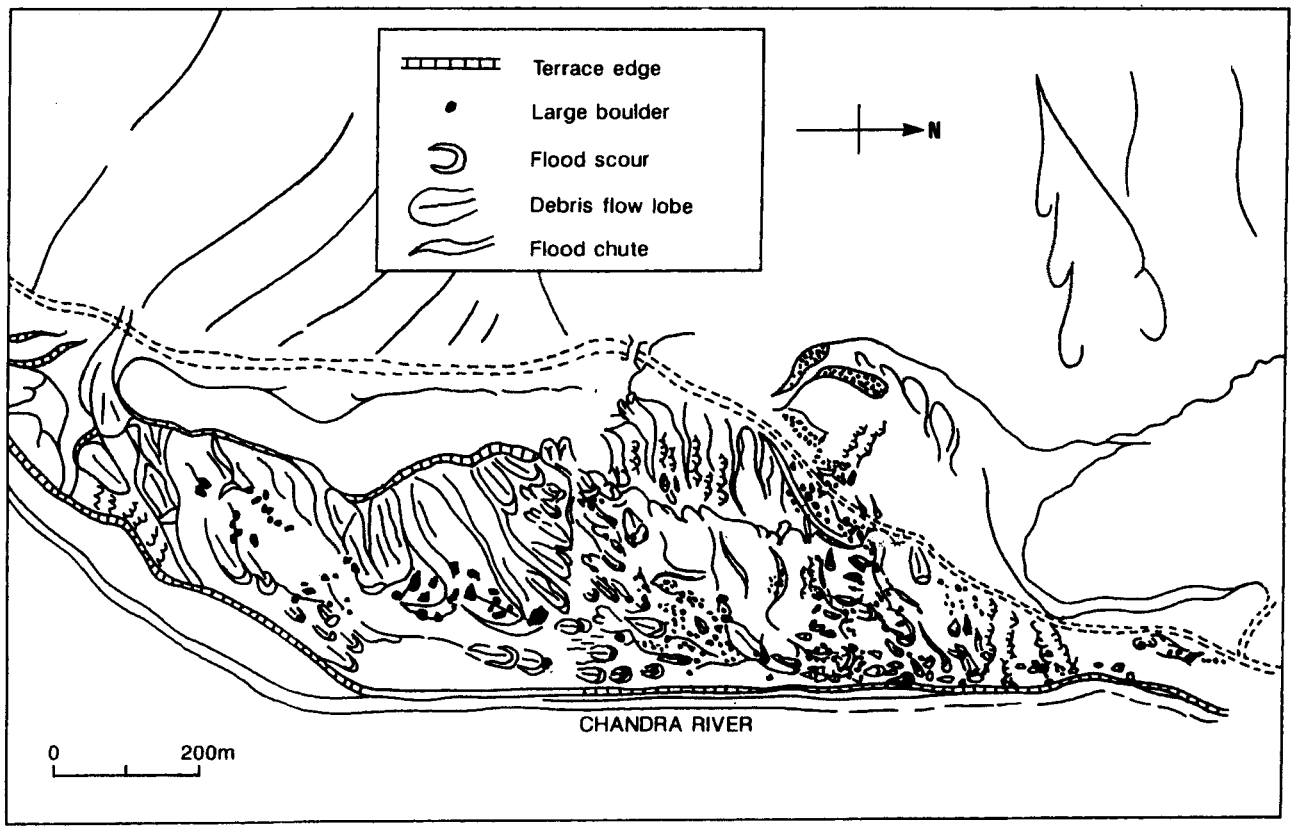

Figure 2 Geomorphological map of the area south of the Batal Bridge showing the detailed sedimentary structures and bedforms produced by the Batal flood. D in Fig. 1 shows the location of this area.

(ii) This surface has imbricate boulder clusters, some of which are very large with long sediment tails and scours (Figs 2 and 6). The largest clast sizes (mean diameter $(LIS)^{0.3}$) are approximately 2.2 m (area 1, Fig. 6).

(iii) This comprises a bar of large boulders and cobbles which rises to approximately 1–2 m higher than the main terrace. A lenticular bar approximately 500 m long is present in the central part of the terrace. Scours are present (4 m deep, 8 m wide, with tails 50 m long) (Fig. 9D) and the largest clast sizes (mean diameter $(LIS)^{0.3}$) are approximately 2.87 m (area 7, Fig. 6).

The flood deposit between Bara Shigri and Chhatiru is dominated by clusters of imbricated boulders and gravelly chutes (Figs 7 and 9), and occasional scour hollows. In places the flood deposit reaches thicknesses of more than 20 m.

Palaeohydrology

Figure 5 shows a reconstruction of Glacial Lake Batal, based on the elevations of shorelines and deltas. The head of water at the Batal glacial dam was at least 200 m and the minimum volume of water when the lake was at its highest was approximately 1.496 km^3.

The largest-clast data collected along transects in each of the study areas (Table 1) allowed both theoretical calculations of boulder overturning (Helley, 1969; Mears, 1979) and empirical estimates of transport velocity (Costa, 1983) to be used to calculate the dimensions of the flow. The use of largest-clast data in deposits laid down by complex, variable and sediment laden flows is prone to error (e.g. see Maizels, 1983, 1989). Indeed, the calculations used to estimate palaeovelocities and palaeodischarges are based on very limited data sets. However, it is possible to use largest-clast data to estimate the order of magnitude of palaeovelocity and palaeodischarge (Maizels, 1983) and the figures presented here are believed to be realistic estimates. The methods applied have been used widely in reconstructions of other flood events. Appendix 1 shows the equations used in this study and Table 1 shows summarised results. These figures give very consistent velocity (v) values of between 5 and 8 m s^{-1} (Table 1).

Estimates for the cross-sectional area of the flood is difficult because slope modification of strandlines has made calculations of flow depth difficult in most of the study areas. The minimum flow depth, however, can be considered to be at least 4 m (the minimum height of the flood deposit). In addition, the cross-sectional area at Batal can be estimated by the height of fine sediment found in the backwater area (4 m above the terrace). The average width of the valley is approximately 900 m and therefore the cross-section area (A) of the flow was approximately 3600 m^2 (900 m × 4 m). This gives a peak flood discharge (Q) of between 21 000 and 27 000 m^3 s^{-1} ($Q = vA$) at Batal; an average of 24 000 m^3 s^{-1} is realistic. The variable Q estimates downstream of Batal are the result of measuring backwater flows and give a large range of values from Chhatiru. The Batal data, however, are more consistent. Given these discharges and the lake volume, Glacial Lake Batal would have drained as one event lasting 0.76 days (just over 18 h).

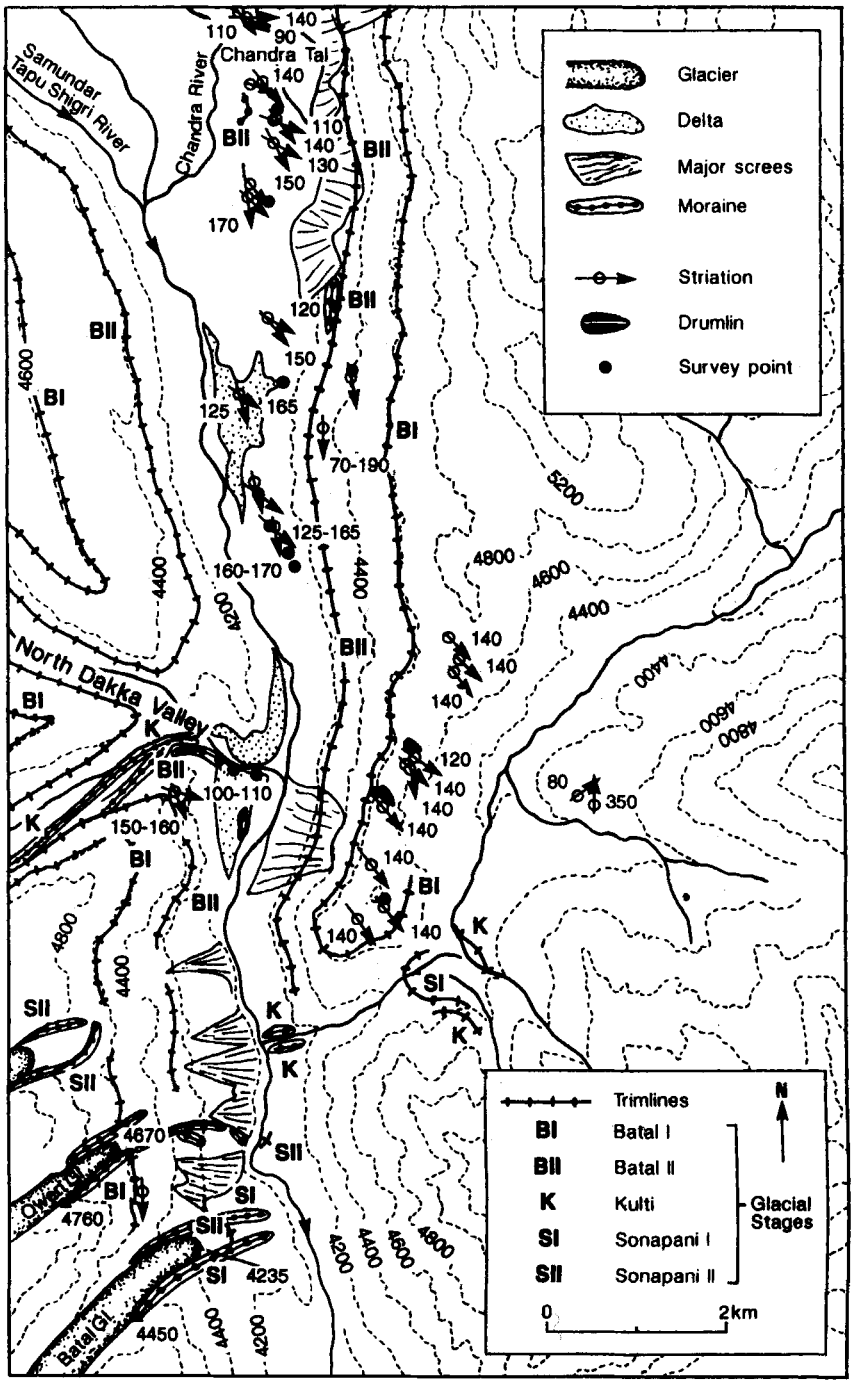

Figure 3 Geomorphological map of the Chandra valley between Batal and Chandra Tal, showing the deltas and shorelines of Glacial Lake Batal.

Discussion – comparison with other floods in the Himalayan Mountains

Tributary glaciers advancing into main valleys have also created dams and subsequent floods in other parts of the Himalayas. Of particular note are those in the Karakoram Mountains in northern Pakistan. These include: the rapid advance of Batura Glacier which dammed the Hunza in the 1770s, ca. 1925, 1972, 1973 and 1974 (Batura Investigation Group, 1976); the rapid advance of Minapin Glacier during 1889–1892 (Mason, 1930); the surge of the Yangutsa Glacier in 1901 (Mason, 1930); the rapid advance of the Hasanabad Glacier in 1903 (Mason, 1930); and advances of various glaciers in the Shimshal valley (including the Mulangutti Glacier) in 1859, 1884, 1893, 1905, 1906, 1927 and 1928 (Mason, 1930). The ice-dam bursts in the Shimshal valley, a tributary valley of the Hunza, were considerable in size. A 3-m rise in river level caused considerable damage to the villages of Ganesh and Baltit in the Hunza valley, some 70 km down-valley from the dam in the Shimshal valley; this occurred in 1884. Similar events followed, with floodwaves 9 m and 15 m high flowing down the Hunza in 1905 and 1906 respectively. In 1959, Finsterwalder (1959) recorded a sudden outburst from an ice-dammed lake in the Shimshal valley, which caused a flood wave of approximately 30 m to be produced, destroying the village of Pasu at the confluence with the Hunza River, approximately 40 km down-valley. Desio and Orombelli (1971) and Goudie *et al.* (1984) recognised extensive lacustrine terraces along the middle

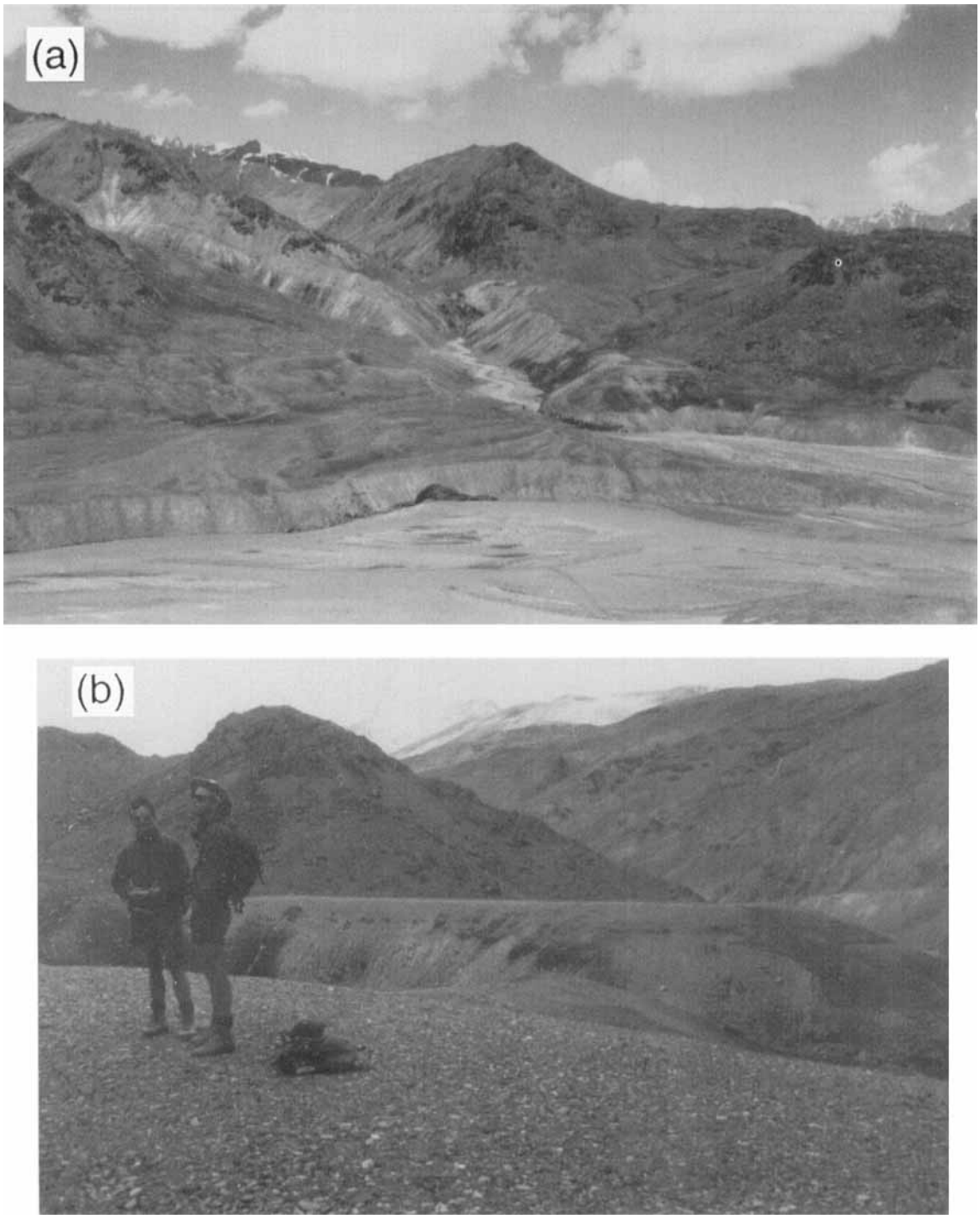

Figure 4 (A) View of deltas and shorelines looking northwest across the Chandra valley towards the North Dakka valley. The line marked s-s shows the highest delta level and shoreline. (B) View of the deltas at the confluence of the South Dakka and Chandra valleys showing the washed delta surface.

Indus and Hunza valleys, respectively, which they attributed to lakes that formed as tributary valley glaciers advanced into the main trunk valleys during the Last Glacial, damming the valley to form a series of lakes. These would have had the potential to burst catastrophically, yet no flood deposits have been recognised, with the exception of the so called Punjab erratics (Desio and Orombelli, 1971). The largest known glacial lake outburst in the Himalayas occurred some 600 yr ago in the vicinity of Pokhara, Nepal, and deposited approximately 5.5 km^3 of debris (Fort and Freytet, 1982).

In Nepal, a moraine-dammed lake drained catastrophically on 5 August 1985 in a tributary valley of the Bhote Kosi (Langmoche Glacier: Galay, 1986; Ives, 1986; Vuichard and Zimmermann, 1986, 1987) provided the opportunity to assess the environmental effects of such a flood and prompted a preliminary enquiry into the recurrence interval of such events (Ives and Messerli, 1989). In the Khumbu Himal at least three glacial outbursts, and possibly five have occurred within living memory (Ives and Messerli, 1989; Vuichard and Zimmermann, 1986). Vuichard and Zimmermann (1986) developed a sediment budget for the outburst and concluded that most of the material was resedimented within about 25 km in the stream channel and only about 10–15% (finer fraction) was transported out of the area. They showed that 900 000 m^3 of material was removed from the moraine dam and most was redeposited within 2 km of

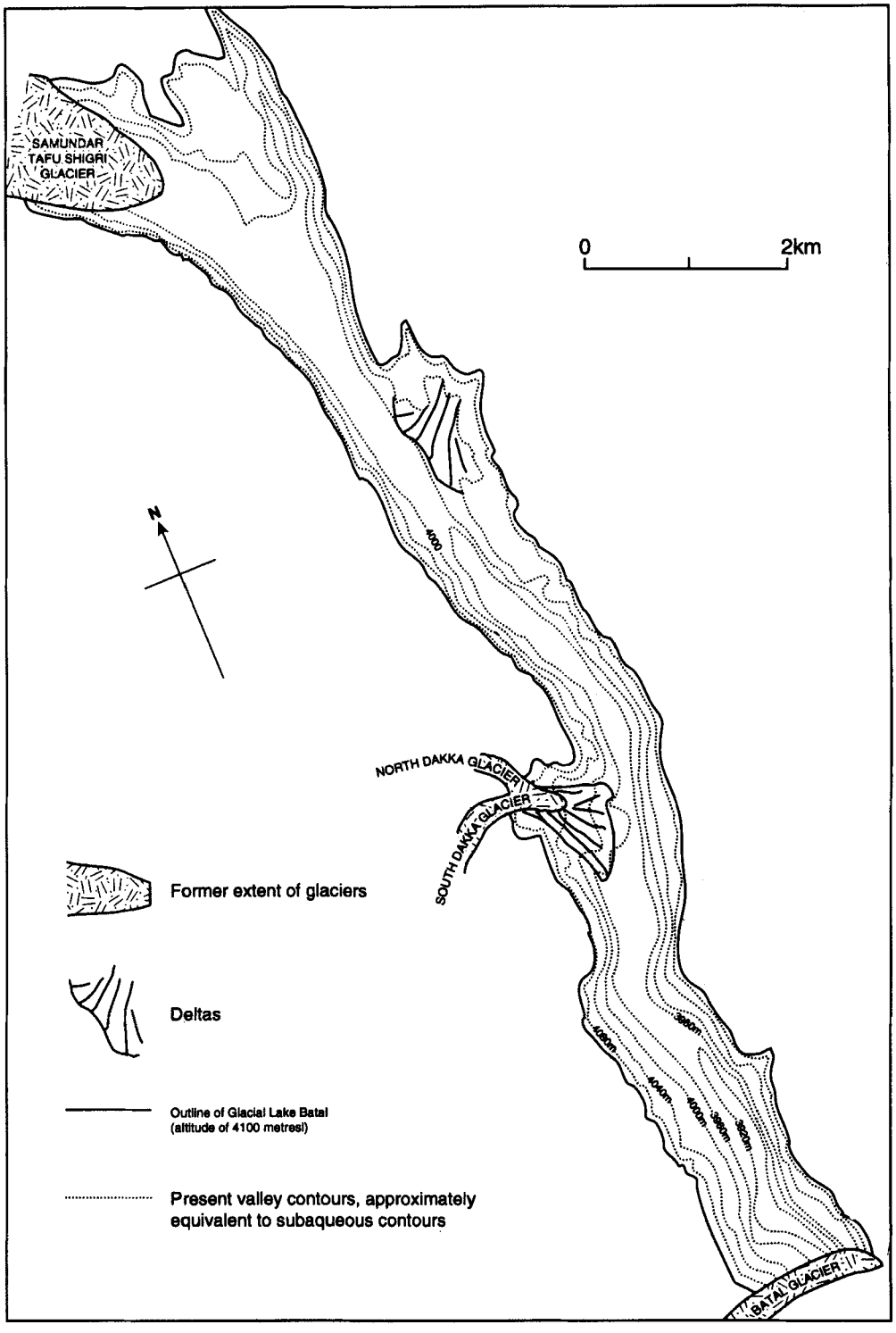

Figure 5 Reconstruction of Glacial Lake Batal showing the former positions of glaciers and deltas.

the breach. Much more material was picked up from the stream channel and the valley sides further down the valley. The peak discharge was calculated at 1600 m^3 s^{-1} about 3 km from the breach and the flow attenuated downstream.

Few studies have, however, reconstructed the peak flood discharges accurately. The best Himalayan example is the Chong Kumdan (Shyok River) in India in 1929 for which Gunn (1930) and Hewitt (1982) have calculated the dam height to have been 120 m and the volume of the lake to be 1350×10^6 m^3, with a peak discharge of approximately 22 650 m^3 s^{-1}. Elsewhere in the world, many glacial dam bursts have had much lower discharges, as is illustrated in Fig. 10, although some (Baker *et al.*, 1993) have been considerably larger.

Catastrophic floods in the Himalaya can also be produced by other mechanisms, including the burst of landslide dammed lakes and intense monsoonal rains. One of the most famous floods occurred in 1858, six months after a landslide blocked the Hunza River at Phungurh. Upon bursting a catastrophic flood-wave advanced down the Indus, raising the river level at Attock in the Punjab by some 9 m in less than 10 h. The volume of water drained may well have been over 1×10^6 m^3 (Mason, 1929; Belcher, 1859). In 1841, a large rockslide dam blocked the Indus River at

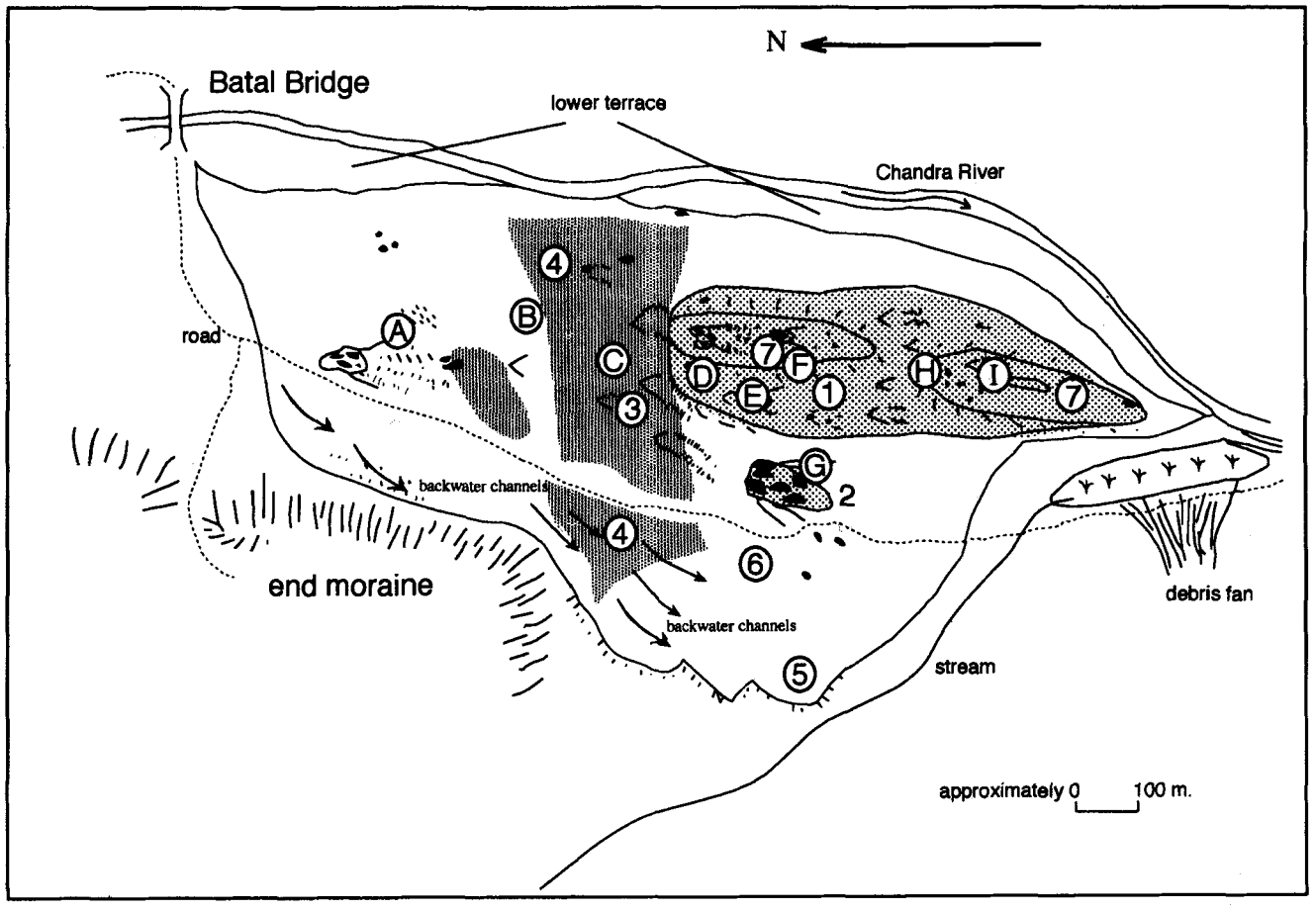

Figure 6 Simplified geomorphology map of the Batal main flood terrace showing the main regions and sampling points. (1) Central flood bar showing large imbricated boulder clusters and deep scour hollows. High volumes of large clasts are scattered across the surface. (2) A stack of large imbricated boulders with a long deposition tail and two adjacent elongate scour hollows. (3) Large scour hollows (deeper than 3 m) which become common downstream of this point. (4) Large ripple troughs (shaded area). Their amplitude is generally < 1 m (60–70 cm is common) and the wavelength is 7–10 m and up to 17 m. The clasts are cobble sized in a matrix of gravel, but there are frequent boulders lying on the surface and large-scale interference of the ripple patterns from deep scours and ridges downstream of the boulders. Figure 9 shows students standing in the ripple troughs: (5) Backwater area of the flood flow with fine sediments reaching 4 m above the highest part of the terrace at 7. (6) An area of coarse imbricate boulder clusters. (7) The highest part of the main flood bar. (A to I refer to the sampling locations for the measurement of the largest clasts transported by the flood flow. The details are given in Table 1).

Lichar on the northeast side of Nanga Parbat. This burst and sent floodwater down the Indus to Attock where it destroyed an Army that was camped on the floodplain (Butler *et al.*, 1988; Owen, 1988; Shroder, 1993). In the Garhwal Himalaya, heavy monsoon rains in 1978 initiated a series of slope failures in the Bhagirathi valley, which temporarily blocked the valley at several locations. These were breached shortly afterwards resulting in a series of catastrophic floods (Prasad and Rawat, 1979). None of these previous studies have calculated the size of past peak-flood discharges reliably. Landslide bursts elsewhere, however, show that the size of past burst-through natural dams (natural dam bursts) and burst-through dams constructed by humans (constructional dam burst) are considerable in size. This is illustrated in Fig. 10 which shows plots for 29 dam failures associated with glacial dams, landslide dams and constructed dams (after Costa, 1985, 1988). Using the equations of Costa (1985, 1988) shown on Fig. 10 for known floods it is possible to compare the Batal flood with results obtained using his empirically derived equations (Table 2). For example his equation for landslide dams on Fig. 10B is 672 volume$^{0.56}$, i.e. $672 \times 1498^{0.56} = 40302$ m^3 s^{-1} (the volume of Glacial Lake Batal was 1.498 km^3), which is a very large discharge. A minimum estimate (given that the floodwaters may have been considerably deeper than we have assumed) of the discharge for the Batal flood calculated from the sedimentology is 24 000 m^3 s^{-1}, which is larger than his glacial examples (Fig. 10 and Table 2). The Batal flood, therefore, with a mean discharge of 24 000 m^3 s^{-1} is similar to landslide dams or exceptionally large glacial ones such as the Chong Kundam flood.

Flooding resulting from heavy rainfall events has been described by Starkel (1972) and Froehlich and Starkel (1987) in the Darjeeling Himalaya, Brunsden *et al.* (1981) in the Low Himalaya of eastern Nepal and Gilmour *et al.* (1987) in the Middle Hills of Nepal. These flood events, however, are small in comparison with landslide dam or constructional dam bursts, e.g. the Tista River in Darjeeling Himalaya regularly has peak discharges of between 1800 and 2500 m^3 s^{-1}, but in 1989 an exceptionally large flood event had a discharge of over 18 000 m^3 s^{-1} (Starkel, 1989). Therefore the Batal flood event is of considerably higher magnitude than any known monsoon-induced flood.

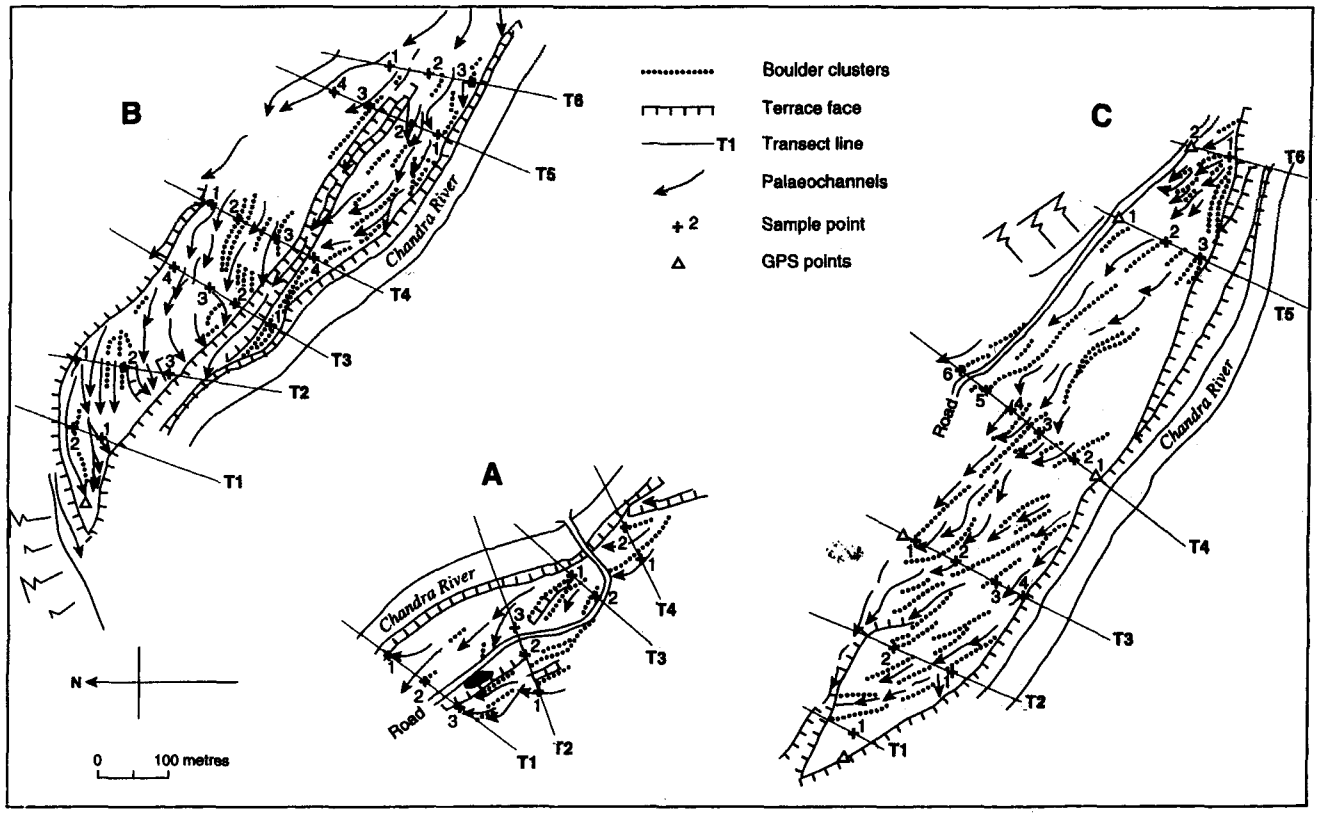

Figure 7 Simplified geomorphological maps of study areas for the lower reaches of the upper Chandra valley. Figure 1 shows the position of these (A, B and C from west to east).

Conclusions

The Batal glacial flood was produced as a result of the catastrophic drainage of Glacial Lake Batal. The large magnitude of the Batal flood event (cf. the work of Costa, 1988; Fig. 10) can be put into a global perspective by comparing it to the superflooding events described by Baker *et al.* (1993), the magnitudes of which far exceed the flood volumes described here. Nevertheless, the Batal flood caused major erosion of glacial moraines and other valley-fill sediments to produce impressive terraces and boulder deposits. The hazard from glacial outburst has been present throughout the Quaternary, although the most likely times for major catastrophic flood are during periods of deglaciation when glacial dams and moraines are readjusting to the new geomorphological regime. This is worrying because presently most glaciers appear to be wasting and retreating throughout the Himalayas (Mayewski and Jeschke, 1979; Mayewski, *et al.*, 1980) and therefore the hazard from lake burst is likely to be on the increase. Hammond (1988), for example, described a dramatic example of a new lake that has formed since 1956 on the lower part of the Imja Glacier below Lhotse. The threat of this lake, which was 0.5 km^2 in extent by 1989, was highlighted by Ives and Messerli (1989). Using metric camera imagery, Ives (1986) showed the presence of at least 50 such ice-dammed and moraine-dammed lakes in the Dudh Kosi and Arun catchments in eastern Nepal and southeastern Xizang. The frequency of breaching of these dams is difficult to assess, but Ives and Messerli (1989) suggest that the recurrence intervals of such events may be small (5–15 yr) and the large number of lakes with the potential to drain catastrophically is impressive. Therefore their role as sediment-transfer and land-forming mechanisms and as hazards is very significant. The extent to which human activity has resulted in land degradation and the extent to which possible global warming has increased the magnitude and frequency of flooding in the Himalayas has not been fully accessed, but some consideration has been given to this in Ives and Messerli (1989), Boughton (1970), Gilmour *et al.* (1987), Hewlett (1982) and Hamilton (1983, 1987). The analysis of flood deposits and a reconstruction of their dynamics is therefore essential for hazard mitigation.

Acknowledgements We should like to thank all the Earthwatch volunteers who contributed to this project, and Earthwatch for their financial and logistical support. Col. Prem Chand of Trans-Himalayan Expeditions (Manali) for his logistical support while in the field. WM would like to thank the University of Luton for financial support. The authors would like to thank Professor V. R. Baker and an anonymous referee for helpful comments on the manuscript.

Appendix

Equations used to calculate palaeovelocity for the flood deposit.

Helley (1969), equation 3

Lift turning arm

$$MR_L = \frac{\beta}{4}\cos\theta + \left(\sqrt{\frac{3}{16}}\alpha^2 \sin\theta\right)$$

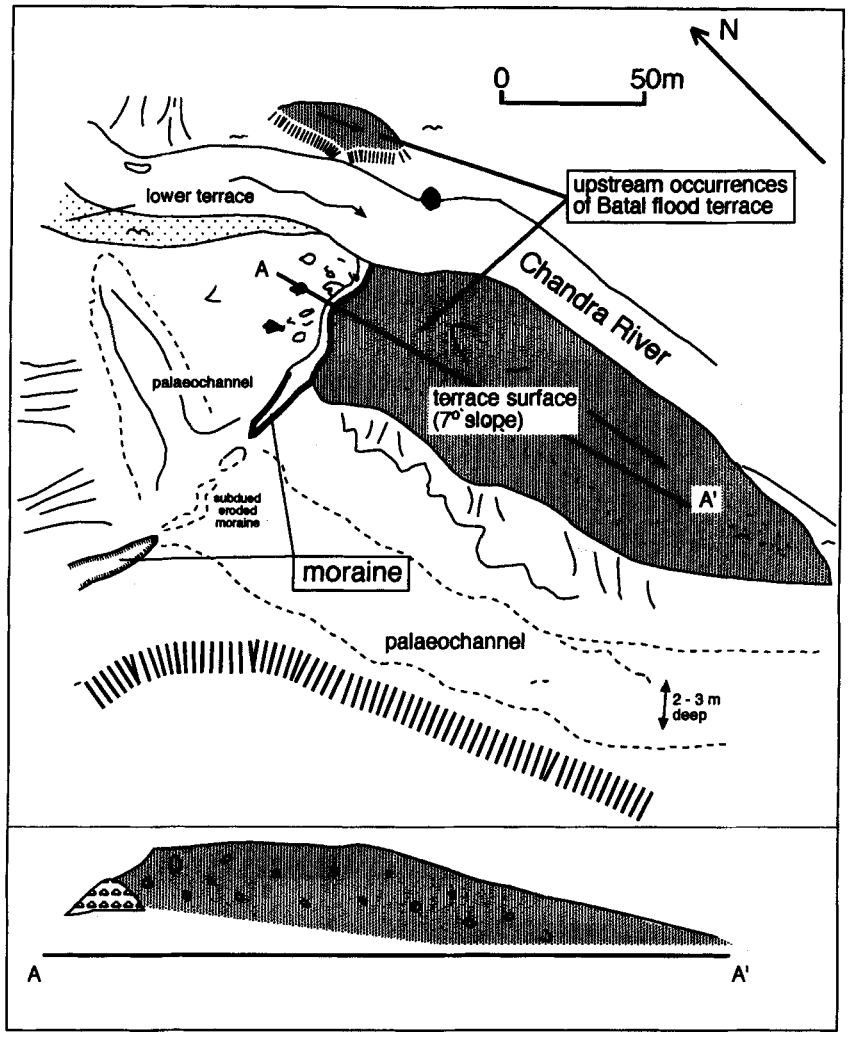

Figure 8 Small terrace, upstream of the Batal Bridge, which has a back channel and moraine crossing the top end of the terrace.

Drag turning arm

$$MR_D = 0.1\alpha \cos\theta + \left(\sqrt{\frac{3}{16}}\alpha^2 \cos\theta - \frac{\beta}{4}\sin\theta\right)$$

Bed velocity (feet per second; fps) at 0.6*a* up from the stream bed (Helley, 1969, equation 3)

$$V_{(0.6\alpha)} = 3.276\sqrt{\frac{(\sigma-1)\gamma(\alpha+\beta)^2(MR_L)}{C_D'\alpha\gamma(MR_D)+0.178\beta\gamma(MR_L)}}$$

Bed velocity (fps) at 0.6α up from the stream bed (Helley, 1969, equation 3 – in full)

$$V_{(0.6\alpha)} = 3.276\sqrt{\frac{(\sigma-1)\gamma(\alpha+\beta)^2\left(\frac{\beta}{4}\cos\theta+\left(\sqrt{\frac{3}{16}}\alpha^2\sin\theta\right)\right)}{C_D'\alpha\gamma\left(0.1\alpha\cos\theta+\left(\sqrt{\frac{3}{16}}\alpha^2\cos\theta-\frac{\beta}{4}\sin\theta\right)\right)+0.178\beta\gamma\left(\frac{\beta}{4}\cos\theta+\left(\sqrt{\frac{3}{16}}\alpha^2\sin\theta\right)\right)}}$$

where $V_{(0.6\alpha)}$ is the bed velocity (fps) at 0.6*a* (values in this paper converted to SI units (m s^{-1})), α is the diameter of the short axis (feet), β the diameter of the intermediate axis (feet), γ the diameter of the long axis (feet), θ is the horizontal angle of imbrication (degrees), σ is the specific gravity of rock (g cm^{-3}), C_D' is the drag coefficient (related to Corey shape factor using Helley, fig. 3, page C4), and the Corey shape factor (after Helley, 1969) = $\alpha\sqrt{\gamma\beta}$.

Mears (1979), equation 7

$$V = \left[\frac{2Dg(1-\tan\beta)(\cos\beta)(\sigma-\rho_f)}{\rho_f C_D}\right]^{0.5}$$

where V is the velocity necessary for overturning clasts (m s^{-1}), D is the average of the long (L), intermediate (I) and short (S) axes of the five largest clasts transported (assumed to be a cubic clast using $(LIS)^{1/3}$), g is the acceleration due to gravity (9.81 m s^{-1} s^{-1}), σ is the specific gravity of the clast (taken by Mears to be 2700 kg m^{-3}), ρ_f is the specific gravity of fluid (taken by Mears to be 1200 kg m^{-3}, to allow for suspended sediment), β is the gradient of the stream bed (degrees), and C_D is the drag coefficient (taken by Mears to be 1.2). Here the value of C_D is calculated from the Corey shape factor and using Helley (1969, fig. 3).

Costa (1983), equation 8

$$\bar{V} = 0.18d_i^{0.455}$$

Table 1 The mean dimensions of the five largest boulders, average flow velocity and estimated discharges along selected transects in the study area. The table shows the average flow velocities calculated using the methods of Costa (1983), Helley (1969) and Mears (1979) – see text. The range is obtained simply by subtracting the V_{min} from the V_{max} calculated using these empirical and theoretical methods. Mean values for measured a, b and c-axes are given, as are the cross-sectional areas of flow and the estimated discharge. The cross-sectional area of the flow has been estimated from the width of the floodplain and the height to which finer sediments accumulated along the valley margin

Site reference	Distance from Batal Bridge (km)	Average flow velocity ($m\ s^{-1}$)	Range of flow velocity ($m\ s^{-1}$)	Mean long axis γ (m)	Mean intermediate axis β (m)	Mean short axis α (m)	Cross-sectional area of flow (m^2)	Estimated discharge ($m^3\ s^{-1}$)
Batal A	0.45	6.2	2.8	2.86	2.20	0.93	3600	22253
Batal B	0.62	6.1	2.3	3.08	1.99	1.15	3600	21781
Batal C	0.77	5.9	2.3	3.02	1.96	0.90	3600	21107
Batal D	0.87	6.6	2.4	3.28	2.30	1.42	3600	23615
Batal E	0.99	7.7	2.6	4.00	3.16	1.88	3600	27745
Batal F	1.10	7.0	3.3	3.92	2.23	2.15	3600	25192
Batal G	1.16	7.1	2.8	4.56	2.92	1.54	3600	25530
Batal H	1.25	6.9	2.7	4.94	2.78	1.35	3600	24974
Batal I	1.34	7.0	2.7	4.48	2.82	1.46	3600	25260
Chhatiru T1.1	19.20	7.3	2.6	4.00	2.72	1.90	3600	26326
Chhatiru T2.1	19.00	7.1	2.5	3.56	2.46	1.86	3600	25411
Chhatiru T2.2	19.00	7.4	3.0	4.92	2.78	2.14	3600	26509
Chhatiru T3.1	18.80	7.6	2.5	3.82	2.76	2.14	3600	27319
Chhatiru T3.2	18.80	7.4	3.0	3.06	2.38	2.12	3600	26738
Chhatiru T3.3	18.80	6.3	2.2	2.66	1.94	1.46	3600	22691
Chhatiru T3.4	18.80	6.4	2.5	3.36	2.06	1.52	3600	22883
Chhatiru T4.1	18.55	5.1	1.9	2.02	1.38	0.84	3600	18479
Chhatiru T4.2	18.55	9.3	3.3	5.34	4.02	3.34	3600	33369
Chhatiru T4.3	18.55	8.7	3.8	4.54	3.28	2.96	3600	31355
Chhatiru T4.4	18.55	6.6	1.3	2.06	1.68	0.80	3600	23743
Chhatiru T4.5	18.55	5.1	1.9	1.86	1.32	0.88	3600	18352
Chhatiru T4.6	18.55	5.1	1.9	1.92	1.32	0.90	3600	18453
Chhatiru T5.1	18.15	5.4	2.0	2.22	1.60	0.82	3600	19448
Chhatiru T5.2	18.15	6.4	2.2	2.78	1.94	1.54	3600	23038
Chhatiru T5.3	18.15	8.0	2.9	4.80	3.32	2.34	3600	28964
Chhatiru T6.1	18.00	5.6	2.0	2.24	1.58	1.04	3600	20112
Chhatiru T6.2	18.00	6.3	2.0	2.38	2.12	1.12	3600	22717
Chhatiru T1.1	29.00	5.4	1.9	2.12	1.48	0.92	3600	19321
Chhatiru T1.2	29.00	3.7	1.5	1.28	0.74	0.40	3600	13305
Chhatiru T2.1	28.80	4.1	1.5	1.26	0.90	0.50	3600	14883
Chhatiru T2.2	28.80	6.5	2.0	2.52	2.00	1.52	3600	23393
Chhatiru T2.3	28.80	5.4	1.8	1.64	1.44	1.00	3600	19551
Chhatiru T3.1	28.60	7.1	2.4	3.56	2.58	1.68	3600	25495
Chhatiru T3.2	28.60	5.5	2.0	2.28	1.60	0.96	3600	19847
Chhatiru T3.3	28.60	7.1	2.4	3.36	2.66	1.68	3600	25733
Chhatiru T3.4	28.60	4.3	1.5	1.08	0.92	0.58	3600	15392
Chhatiru T4.1	28.45	3.7	1.6	1.28	0.74	0.44	3600	13463
Chhatiru T4.2	28.45	7.3	2.5	4.02	2.92	1.56	3600	26257
Chhatiru T4.3	28.45	7.1	2.9	2.84	2.18	1.94	3600	25639
Chhatiru T4.4	28.45	10.9	3.4	7.16	6.34	3.76	3600	39176
Chhatiru T5.1	28.10	7.1	2.5	3.60	2.72	1.60	3600	25660
Chhatiru T5.2	28.10	6.7	2.8	3.68	2.62	1.16	3600	24280
Chhatiru T5.3	28.10	6.9	2.4	3.14	2.42	1.68	3600	24938
Chhatiru T5.4	28.10	4.3	1.5	1.26	1.00	0.52	3600	15603
Chhatiru T6.1	28.00	3.6	1.4	1.06	0.68	0.40	3600	13004
Chhatiru T6.2	28.00	4.8	1.8	1.88	1.28	0.64	3600	17331
Chhatiru T6.3	28.00	6.3	2.3	2.84	1.88	1.56	3600	22813
Near Chhatiru T1.1	31.00	4.1	1.4	1.14	0.88	0.50	3600	14851
Near Chhatiru T1.2	31.00	5.1	2.0	2.16	1.36	0.82	3600	18228
Near Chhatiru T1.3	31.00	5.9	2.2	2.80	1.80	1.18	3600	21184
Near Chhatiru T2.1	30.80	6.9	2.6	4.06	2.64	1.40	3600	24728
Near Chhatiru T2.2	30.80	9.1	3.7	5.02	4.74	2.06	3600	32746
Near Chhatiru T2.3	30.80	4.7	2.0	1.64	1.22	0.52	3600	16798
Near Chhatiru T3.1	30.60	6.7	2.4	3.26	2.42	1.42	3600	24268
Near Chhatiru T3.2	30.60	5.5	1.9	2.02	1.60	0.90	3600	19830
Near Chhatiru T4.1	30.50	5.1	2.0	2.14	1.42	0.74	3600	18255
Near Chhatiru T4.2	30.50	6.9	2.8	4.28	2.72	1.24	3600	24687

Figure 9 Photographs of characteristic features of the flood deposit. (A) Imbricated boulders at Chhatiru. (B) A large scour in the Bata flood terrace located in the vicinity of site 3 on Fig. 6.

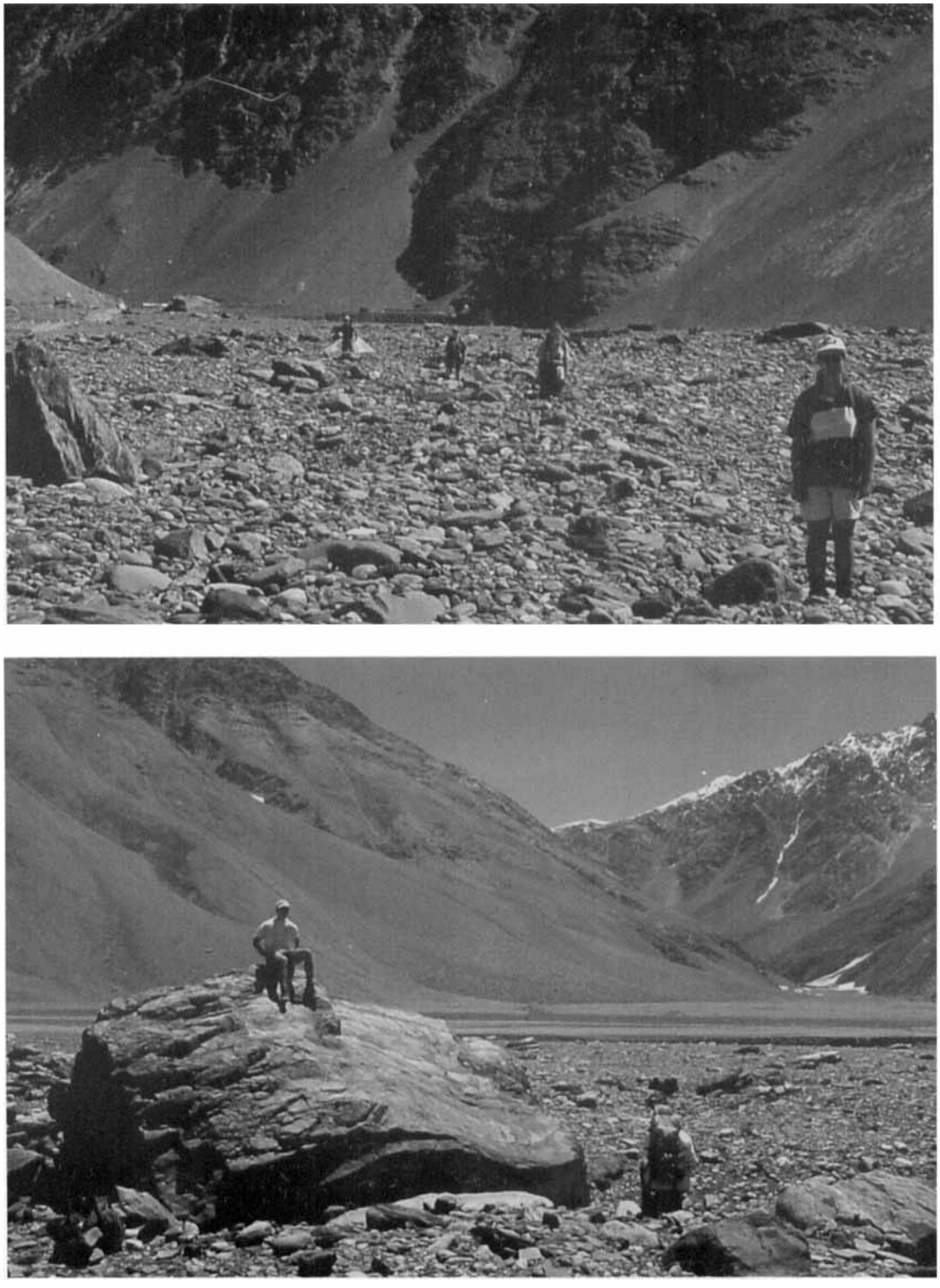

Figure 9 (C) A line of Earthwatch volunteers standing in large ripple troughs in the Batal flood terrace in the shaded area (4) on Fig. 6. The ripple amplitude is generally < 1 m (60–70 cm common) and the wavelength is 7–10 m and up to 17 m. (D) A transported clast on the surface of the Batal flood terrace showing the associated down-flow scour. This clast is from site H on Fig. 6 and measures 8.9 × 4.6 × 2.8 m.

Figure 9 (E) A cluster of large clasts from near site 6 on Fig. 6.

Table 2 The comparison between the dimensions of the Batal dam and those for glacial dams, landslide dams and constructed dams using the empirically derived equations of Costa (1985)

		Q_{max} ($m^3 s^{-1}$) (Costa, 1985, fig. 7)	Q_{max} ($m^3 s^{-1}$) (Costa, 1985, fig. 5)	Q_{max} ($m^3 s^{-1}$) (Costa, 1985, fig. 4)
Dam volume (vol)	$1496\ m^3 \times 10^6$			
Dam height (H) (4100–3900 m)	200 m			
Dam factor ($H \times$ vol) (Costa, 1985)	299200			
Glacial dams		$3.8\ (H \times \text{vol})^{0.61}$	$113\ \text{vol}^{0.64}$	$22\ H^{0.73}$
		8320	12163	1052
Landslide dams		$181\ (H \times \text{vol})^{0.43}$	$672\ \text{vol}^{0.56}$	$6.3\ H^{1.59}$
		40958	40302	28706
Constructed dams		$325\ (H \times \text{vol})^{0.42}$	$961\ \text{vol}^{0.48}$	$10.5\ H^{1.87}$
		64832	3776	210919
Time to empty lake assuming $1.496 \times 10^9\ m^3$ water	$Q = 24 \times 10^3\ m^3\ s^{-1}$ = 0.72 days			

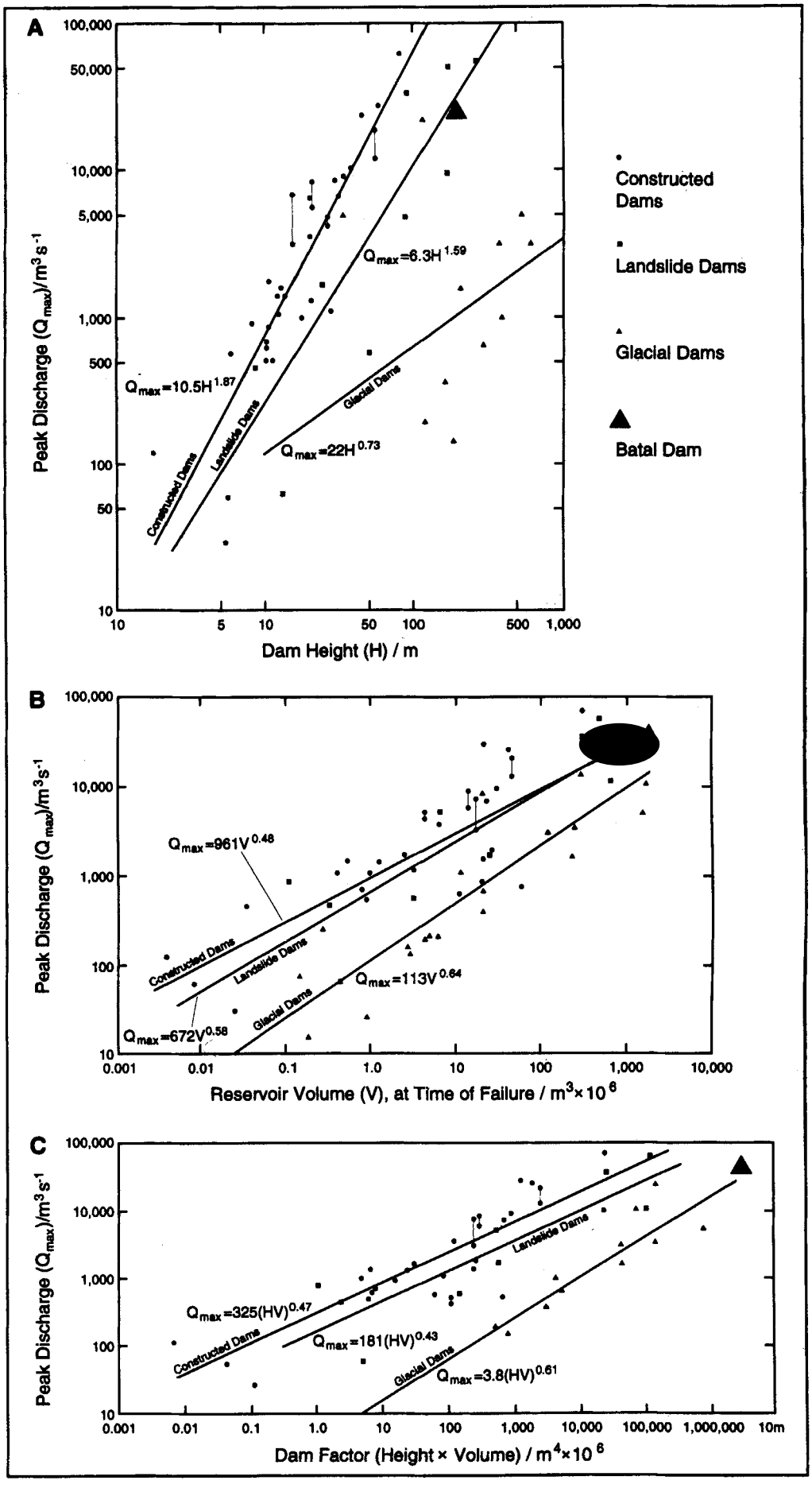

Figure 10 Graphs showing the relationships between: (A) peak discharge against dam height; (B) peak discharge against reservoir volume; and (C) peak discharge against dam factor (height × volume). These are based on a sample of 62 dam failures (after Costa, 1985, 1988). The Batal flood (bold triangle) plots in the landslide envelope.

where $\bar{V}$ is the mean velocity (m s^{-1}) and d_i is the average of the intermediate diameter of the five largest (transported) clasts (m).

Costa (1983), equation 10

$$\bar{V} = 0.18 d_i^{0.487}$$

where $\bar{V}$ is the mean velocity (m s^{-1}) and d_i is the average of the intermediate diameter of the five largest (transported) clasts (m).

References

BAKER, V. R., BENITO, G. and RUDOY, A. N. 1993. Paleohydrology of Late Pleistocene superflooding, Altay Mountains, Siberia. *Science,* **259**, 348–350.

BATURA INVESTIGATION GROUP 1976. *Investigation Report on the Batura Glacier in the Karakoram Mountains, the Islamic Republic of Pakistan* (1974–1975). Peking, 51 pp.

BELCHER, J. 1859. Letter addressed to R. H. Davies, Esquire. Secretary to the Government of the Punjab and its dependencies. *Journal of the Asiatic Society of Bengal,* **28**, 219–228.

BOUGHTON, W. C. 1970. *Effects of Land Management on Quantity and Quality of Available Water. New South Wales, Australia.* University of New South Wales, Water Research Laboratory Report, No. 120.

BRUNSDEN, D., JONES, D. K., MARTIN, R. P. and DOORNKAMP, J. C. 1981. The geomorphological character of part of the Low Himalaya of eastern Nepal. *Zeitschrift für Geomorphologie,* **37**, 25–72.

BURBANK, D. W. 1983. Multiple episodes of catastrophic flooding in the Peshawar Basin during the past 700 000 years. *Geological Bulletin of the University of Peshawar,* **16**, 43–49.

BUTLER, R. W. H., OWEN, L. A. and PRIOR, D. J. 1988. Flash-floods, earthquakes and uplift in the Pakistan Himalayas. *Geology Today,* **4**(6), 197–201.

COSTA, J. E. 1983. Paleohydraulic reconstruction of flash-flood peaks from boulder deposits in the Colorado Front Range. *Geological Society of America Bulletin,* **94**, 986–1004.

COSTA, J. E. 1985. *Floods from Dam Failures.* US Geological Survey, Open-File Report 85–560.

COSTA, J. E. (1988): *Floods from Dam Failures. IN*: Baker, V. R., Kochel, R. C. and Patton, P. C. (eds), *Flood Geomorphology,* 439–463. Wiley, Chichester.

DESIO, A. and OROMBELLI, G. 1971. Preliminary note on the presence of a large valley glacier in the middle Indus Valley (Pakistan) during the Pleistocene. *Atti della Accademia Nazionale dei Lincei,* **51**, 387–392 (in Italian).

DESIO, A. and OROMBELLI, G. 1983. The 'Punjab erratics' and the maximum extent of the glaciers in the middle Indus valley (Pakistan) during the Pleistocene. *Atti della Accademia Nazionale dei Lincei,* Series 8, **17**(179), 135–180.

FORT, M. B. and FREYTET, P. 1982. The Quaternary sedimentary evolution of the intra-montane basin of Pokhara in relation to the Himalaya Midlands and their hinterland (West Central Nepal). *IN*: Sinha, A. K. (ed.), *Contemporary Geoscientific Researches in Himalaya,* Vol. 2, 91–96. Dehra Dun, India.

FINSTERWALDER, R. 1959. Recent German expeditions to the Batura Mustagh and Rakaposhi. *Journal of Glaciology,* **3**, 787.

FROEHLICH, W. and STARKEL, L. 1987. Normal and extreme monsoon rains – their role in the shaping of the Darjeeling Himalaya. *Studia Geomorphologica Carpatho-Balcanica,* **21**, 129–160.

GALAY, V. 1986. *Glacier Lake Outburst Flood (Jökulhlaup) on the Bhote/Dudh Kosi – August 4, 1985.* Internal Report, Water and Energy Commission, Kathmandu.

GANSSER, A. 1966. Geological research in the Bhutan Himalaya. *IN: Mountain World 1964/1965.* Swiss Foundation for Alpine Research, Zurich.

GILMOUR, D. A., BONELL, M. and CASSELLS, D. S. 1987. The effects of forestation on soil hydrolaulic properties in the Middle Hills of Nepal: a preliminary assessment. *Mountain Research and Development,* **7**(3), 239–249.

GOUDIE, A. S., BRUNSDEN, D., COLLINS, D. N., DERBYSHIRE, E., FERGUSON, R. I., HASHNET, Z., JONES, D. K. C., PERROTT, F. A., SAID, M., WATERS, R. S. and WHALLEY, W. B. 1984. The geomorphology of the Hunza Valley, Karakoram Mountains, Pakistan. *IN:* Miller, K. (ed.), *International Karakoram Project,* 359–411. Cambridge University Press, Cambridge.

GUNN, J. P. 1930. The Shyok flood, 1929. *Himalayan Journal,* **2**, 35–47.

HAGEN, T., DYHRENFURTH, G-O, von FÜRER-HAIMENDORF, C. and SCHNEIDER, E. (1963): *Mount Everest. Formation, Population and Exploration of the Everest Region.* (translated by E. N. Bowman). Oxford University Press, London.

HAMILTON, L. S. 1983 (eds). *Forest and Watershed Development and Conservation in Asia and the Pacific.* Westview Press, Boulder, Colorado.

HAMILTON, L. S. 1987. What are the impacts of Himalayan deforestation on the Ganges–Brahmaputra lowlands and delta? Assumptions and facts. *Mountain Research and Development,* **7**(3), 256–263.

HAMMOND, J. E. 1988. *Glacial lakes in the Khumbu Region, Nepal: an assessment of the hazards.* Unpublished Master's thesis, University of Colorado, Boulder.

HELLEY, E. J. 1969. Field measurement of the initiation of large bed particle motion in Blue Creek near Klamath, California. *Geological Survey Professional Paper,* **562-G**, 19 pp.

HEWITT, K. 1964. A Karakoram ice dam. *Industrial Journal of Water and Power Develelopment Authority (Pakistan),* **5**, 18–30.

HEWITT, K. 1982. Natural dams and outburst floods of the Karakoram Himalaya. *IN*: J. W. Glen (ed.), *Hydrological aspects of Alpine and High Mountain Areas,* 259–269. International Association of Hydrological Scientists, Publication No. 138. Washington, IAHS.

HEWLETT, J. D. 1982. Forests and floods in the light of recent investigations. *IN: Proceedeedings of the Hydrological Symposium, 14–15 June 1982, Fredericton,* 543–560. National Research Council, Canada.

IVES, J. D. 1986. *Glacial lake outburst floods and risk engineering in the Himalaya.* Occasional Paper No. 5. International Centre for Integrated Mountain Development (ICIMOD), Kathmandu.

IVES, J. D. and MESSERLI, B. 1989. *The Himalayan Dilemma.* Routledge, London.

MAIZELS, J. K. 1983. Palaeovelocity and palaeodischarge determination for coarse gravel deposits. *IN*: Gregory, K. J. (ed.), *Background to Palaeohydrology,* 101–140. Wiley, Chichester.

MAIZELS, J. K. 1989. Sedimentology, palaeoflow dynamics and flood history of jökulhlaup deposits: palaeohydrology of Holocene sediment sequences in southern Iceland sandur deposits. *Journal of Sedimentary Petrology,* **59**, 204–223.

MASON, K. 1929. The representation of glaciated regions on maps of the survey of India. *Geological Survey of India, Professional Paper,* **25**, 18 pp.

MASON, K. 1930. The glaciers of the Karakoram and neighbourhood. *Records of the Geological Survey of India,* **63**, 214–278.

MAYEWSKI, P. A. and JESCHKE, P. A. 1979. Himalayan and Trans-Himalayan glacier fluctuations since AD 1812. *Arctic and Alpine Research,* **11**(3), 267–287.

MAYEWSKI, P. A., PREGENT, G. P., JESCHKE, P. A. and AHMED, N. 1980. Himalayan and Trans-Himalayan glacier fluctuations and the south Asian Monsoon Record. *Arctic and Alpine Research,* **12**(2), 171–182.

MEARS, A. I. 1979. Flooding and sediment transport in a small alpine drainage basin in Colorado. *Geology,* **7**, 53–57.

OWEN, L. A. 1988. Neotectonics and glacial deformation in the Karakoram Mountains and Nanga Parbat Himalaya. *Tectonophysics,* **163**, 227–265.

OWEN, L. A., BENN, D. I., DERBYSHIRE, E., EVANS, D. J. A., MITCHELL, W. A. and RICHARDSON, S. 1996. The Quaternary glacial history of the Lahul Himalaya, Northern India. *Journal of Quaternary Science,* **11**, 25–42.

PRASAD, C. and RAWAT, G. S. 1979. Bhagirathi flash-floods, a geomorphological appraisal. *IN*: Sinha, A. K. (ed.), *Himalayan Geology,* 9 (II) WING, 734–743. Dehra Dun, India.

SHRODER, J. F. 1993. Himalaya to the Sea: Geomorphology and the Quaternary of Pakistan in the regional context. *IN*: Shroder, J. F. (ed.), *Himalayas to the Sea: Geology, Geomorphology and the Quaternary,* 108–131. Routledge, London.

STARKEL, L. 1972. The role of catastrophic rainfall in the shaping of the relief of the Lower Himalaya (Darjeeling Hills). *Geographia Polonica,* **21**, 103–147.

STARKEL, L. (1989). Valley floor evolution in the marginal areas of the Himalaya Mountains and the Khasi-Jaintia Plateau. *Zeitschrift für Geomorphologie.* **76**, 1–8.

VUICHARD, D. and ZIMMERMANN, M. 1986. The Langmoche flash-flood, Khumbu Himal, Nepal. *Mountain Research and Development,* **6**(1), 90–94.

VUICHARD, D. and ZIMMERMANN, M. 1987. The catastrophic drainage of a moraine-dammed lake, Khumbu Himal, Nepal: cause and consequences. *Mountain Research and Development,* **7**(2), 91–110.

XU, D. 1985. *Characteristics of debris flows caused by outburst of a glacial lake in the Boqu River in Xizang, China, 1981.* Institute of Glaciology and Cryopedology, Academic Sinica, Lanzhou, Unpublished manuscript, 24 pp.